



HAL
open science

Anatomo-clinical atlases correlate clinical data and electrode contact coordinates: application to subthalamic deep brain stimulation.

Florent Lalys, Claire Haegelen, Mehri Maroua, Sophie Drapier, Marc Verin,
Pierre Jannin

► To cite this version:

Florent Lalys, Claire Haegelen, Mehri Maroua, Sophie Drapier, Marc Verin, et al.. Anatomo-clinical atlases correlate clinical data and electrode contact coordinates: application to subthalamic deep brain stimulation.. *Journal of Neuroscience Methods*, 2013, 212 (2), pp.297-307. 10.1016/j.jneumeth.2012.11.002 . inserm-00750921

HAL Id: inserm-00750921

<https://inserm.hal.science/inserm-00750921>

Submitted on 15 Nov 2012

HAL is a multi-disciplinary open access archive for the deposit and dissemination of scientific research documents, whether they are published or not. The documents may come from teaching and research institutions in France or abroad, or from public or private research centers.

L'archive ouverte pluridisciplinaire **HAL**, est destinée au dépôt et à la diffusion de documents scientifiques de niveau recherche, publiés ou non, émanant des établissements d'enseignement et de recherche français ou étrangers, des laboratoires publics ou privés.

Accepted Manuscript

Title: Anatomico-clinical atlases correlate clinical data and electrode contact coordinates: Application to subthalamic deep brain stimulation

Authors: Florent Lalys, Claire Haegelen, Maroua Mehri, Sophie Drapier, Marc Vérin, Pierre Jannin



PII: S0165-0270(12)00449-9
DOI: doi:10.1016/j.jneumeth.2012.11.002
Reference: NSM 6500

To appear in: *Journal of Neuroscience Methods*

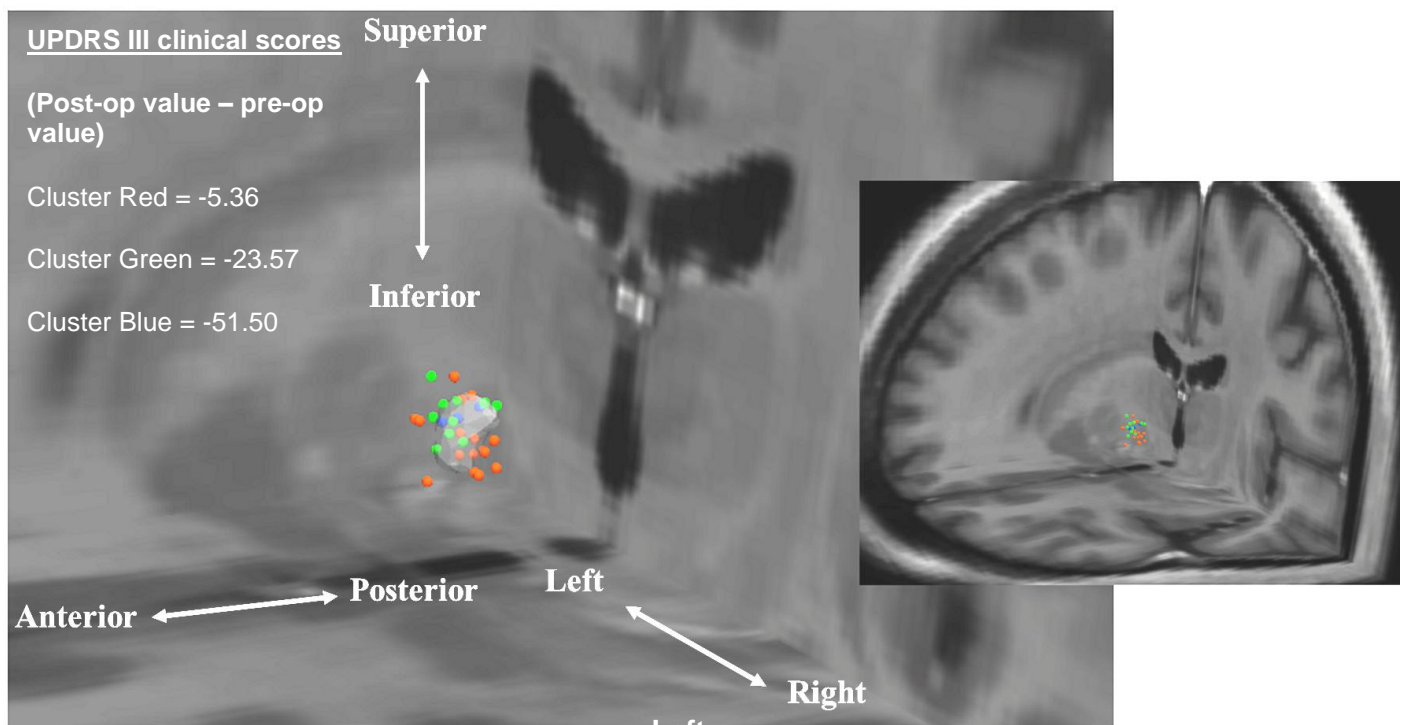
Received date: 28-8-2012
Revised date: 31-10-2012
Accepted date: 2-11-2012

Please cite this article as: Lalys F, Haegelen C, Mehri M, Drapier S, Vérin M, Jannin P, Anatomico-clinical atlases correlate clinical data and electrode contact coordinates: application to subthalamic deep brain stimulation, *Journal of Neuroscience Methods* (2010), doi:10.1016/j.jneumeth.2012.11.002

This is a PDF file of an unedited manuscript that has been accepted for publication. As a service to our customers we are providing this early version of the manuscript. The manuscript will undergo copyediting, typesetting, and review of the resulting proof before it is published in its final form. Please note that during the production process errors may be discovered which could affect the content, and all legal disclaimers that apply to the journal pertain.

Rennes, mercredi, 31 octobre 2012

Graphical abstract :





Unité/Projet VisAGeS U746 • INSERM/INRIA/CNRS/Université de Rennes I

2, Avenue du Pr. Léon Bernard CS34317 35043 Rennes Cedex France • <http://www.irisa.fr/visages>

Rennes, mardi, 28 août 2012

Highlights :

- Creation of anatomo-clinical atlases for SubThalamic Deep Brain Stimulation
- Atlases enable extraction of representative clusters to determine the optimum site
- Atlases help acquire a better understanding of functional mapping in deep structures

Abstract

For patients suffering from Parkinson's disease with severe movement disorders, functional surgery may be required when medical therapy isn't effective. In Deep Brain Stimulation (DBS), electrodes are implanted
5 within the brain to stimulate deep structures such as SubThalamic Nucleus (STN). The quality of patient surgical outcome is generally related to the accuracy of nucleus targeting during surgery. In this paper, we focused on identifying optimum sites for STN DBS by studying symptomatic motor improvement along with neuropsychological side effects. We described successive steps for constructing digital atlases gathering patient's location of electrode contacts automatically segmented from postoperative images, and
10 clinical scores. Three motor and five neuropsychological scores were included in the study. Correlations with active contact locations were carried out using an adapted hierarchical ascendant classification. Such analysis enabled the extraction of representative clusters to determine the optimum site for therapeutic STN DBS. For each clinical score, we built an anatomo-clinical atlas representing its improvement or deterioration in relation with the anatomical location of electrodes and from a population of implanted
15 patients. To our knowledge, we reported for the first time a discrepancy between a very good motor improvement by targeting the postero-superior region of the STN and an inevitable deterioration of the categorical and phonemic fluency in the same region. Such atlases and associated analysis may help better understanding of functional mapping in deep structures and may help pre-operative decision-making process and especially targeting.

20 *Keywords*

Deep brain stimulation, Parkinson disease, anatomo-clinical atlas, medical imaging

25 **1. Introduction**

1.1 Background

Parkinson's Disease (PD) is recognized as one of the most common neurological disorders, affecting 1% of
30 people over the age of 60 years. It is the second most prevalent neurodegenerative disorder. One of the characters of PD is the apoptosis of the dopamine-rich neurons of the substantia nigra. Major symptoms are indeed characterized by abnormalities of motor functions, several of which predominate, but all do not

necessarily occur in all individuals. While these PD-related symptoms can be treated with medical therapy, when it remains ineffective for some patients, a Deep Brain Stimulation (DBS) surgery (Benabid et al., 2000; Krack et al., 2003) might be necessary according to strict patient inclusion criteria. This iterative procedure, initially approved by the Federal Drug Agency in U.S. in 1997 for essential tremor disorders, and in 2002 for PD, has gained much interest over the past decade and is now widely used by a large number of neurosurgical departments. The DBS anatomical target is based on the relief of symptoms and results of previous implantations only. The three major targets chosen by neurosurgeons according to the patients' symptoms are the Caudal part of the Vento-Lateral thalamic nucleus (VLc), the medial Global Pallidus (GPm) and the Sub-Thalamic Nucleus (STN). Among these three deep brain structures, the STN became the most common target of high-frequency DBS in patients with severe motor disabled symptoms and no cognitive impairment (Benabid et al., 2000; Lang and Lozano, 1998; Hamani et al., 2003; Bardinet et al., 2009; Volkmann et al., 2009).

45

1.2 Surgical procedure

During routine DBS surgery, two stages are mainly involved: pre-operative planning and the surgery itself. Pre-operative planning is the process of loading pre-operative patient's medical images (such as Computed Tomography and/or Magnetic Resonance Images), registering them together and proposing a 2D and/or 3D visualisation interface to define the target localisation in the Anterior and Posterior Commissures (AC-PC) plan. Mainly due to contrast and spatial resolutions limitations, the usual DBS targets are not easily visible on the MR images available to the surgeon, even though MRI offers better contrast than other medical imaging techniques (Dormont et al., 2010). Neurosurgeons directly localize the optimal target position on the T2 MR image and choose the trajectory of the electrode on patient's anatomical information. During this step, the additional help of an atlas may be necessary. In practice, experts manually localize AC-PC coordinates, midsagittal points and entry on the MR images of the patient. Finally, coordinates are automatically put in AC-PC space, then computed in a stereotactic coordinates system.

The surgical procedure is then performed under local anaesthesia. The trajectory estimated during planning is implemented with stereotactic frame based or frameless systems and used as an initial position that has to be refined. A few causes of discrepancy between chosen target and the final implant might appear, such as brain shift (Khan et al., 2008; Pallavaram et al., 2009), or patient's anatomical variability.

An X-ray control is thus performed intra-operatively to confirm the initial placement and evaluate potential biases. Electrophysiological explorations are also performed to help neurosurgeons refine the placement of active electrode contacts. Similarly, neurologists may test the clinical effects with different settings for each contact to reach optimum placement. Changing frequency, voltage, stimulated contact and electrode trajectory, they reach optimum placement. Lastly, the surgeon anchors the electrode to the skull.

Even though STN DBS has demonstrated its efficiency for motor symptom improvement, questions remain concerning contact location providing the greatest motor improvement while producing the minimal neuropsychological and psychiatric side effects. Indeed, despite satisfactory motor improvements, several studies have reported adverse-events after DBS surgery affecting cognitive functions, emotion or behaviour (Parsons et al., 2006; Temel et al., 2006; Biseul et al., 2005; Dujardin et al., 2004; Houeto et al., 2002). In particular, Brücke et al. (2007), Kühn et al. (2005), Greenhouse et al. (2011), LHommée et al. (2012) or Mallet et al. (2007) elucidated the role of STN in emotional processing, showing that STN DBS leads to behavioral complications. Similarly, Burrows et al. (2011) were interested in complications of STN DBS around the zona incerta, and York et al. (2009) looked at neuropsychological complications according to electrode location and trajectory. All these results suggest that the STN forms part of a broadly distributed neural network encompassing the associative and limbic circuits. Similarly, Witt et al. (2008) studied neuropsychiatric consequences of STN DBS. Based on this hypothesis, new works have then emerged. For instance, Karachi et al. (2005), or more recently Lambert et al. (2012) supported the hypothesis that the nucleus was separated in three regions: the limbic, associative and motor regions. Similarly, Lenglet et al. (2012) studied the basal ganglia and thalamic connections using high-resolution MR images. As outlined above, one of the major challenges in DBS is the identification of the target, which requires additional information and knowledge for indirect identification of such small structures during the pre-operative stage with the support of digital atlases.

1.3 Atlases

Brain atlases and atlas-based segmentation techniques have been developed to facilitate the accurate targeting of deep brain structures in patients with movement disorders (Schaltenbrand nad Wahren, 1977; Talairach and Tournoux, 1988, Chakravarty, 2006; Yelnik, 2006; Bardinet, 2009; Lalys, 2010). Some

digitized atlases aim at providing information with optimum spatial and intensity resolution, to allow better
95 identification of structures, which is impossible with usual medical imaging techniques only. Histological
atlases were thus created (Yelnik et al., 2007; Chakravarty et al., 2006) along with high-resolution MR
based atlases (Aubert-Broche et al., 2006; Lalys et al., 2011). Both types of atlas have been successfully
introduced in the targeting stage of standard DBS procedures.

The concept of probabilistic functional atlases, built from a population of previous surgical cases, was
100 initially introduced by Nowinski et al. (2003, 2005, 2007). After a step of normalization within a common
space, effective contacts are linked to preoperative electrophysiological recordings and clinical scores
acquired during the stages of the procedure. Statistical techniques are used to study anatomical or functional
variability between patients. Response to stimulation, electro-physiological recordings and clinical scores
related to motor or cognitive evolution are all potential data that can be integrated into such atlases. This
105 fusion of clinical and anatomical information allows an understanding of functional organization within
deep-brain structures that helps in the identification of the optimal therapy zone for further patients. Finnis
et al. (2003) and Guo et al. (2006) proposed probabilistic functional atlases by integrating intra-operative
recordings. D'Haese et al. (2005, 2006) and Pallavaram et al. (2008, 2009) proposed a system to
automatically predict the optimum target position according to atlases built from retrospective studies.
110 More recently, D'Haese et al. (2010) proposed a fully integrated computer-assisted system called
CRAnialVault. The system addresses the issue of data administration between the different stages of the
therapy. It permits the centralization of various types of data acquired during the procedure and provides
data visualisation through data processing tools. A preliminary validation process in a clinical context, from
planning to programming, is described and shows that the system provides genuine assistance to the
115 surgical team.

Evaluation of DBS electrode implantation involves significant neurological and psychological follow-up
estimated by clinical tests. Resulting clinical scores allow post-operative evaluation of the decrease in
motor disorders and possible clinical side effects. Quantitative analysis of these data relative to the actual
stimulated anatomical area would provide a better understanding of the DBS phenomenon, optimisation of
120 targeting and consequently better patient outcome.

As far as we know, no atlases have yet been proposed for representing the relationships between the

STN anatomy and a broad panel of pre- and post-operative clinical scores. While most of these atlases use a single motor score for modelling the global outcome of the patient (e.g. Guo et al., 2006), we proposed in this paper to extend this research by adding pre- and post-operative motor, cognitive and neuropsychological scores of patients with Parkinson's disease and inclusion criteria for subthalamic stimulation. We thus introduce the concept of anatomo-clinical atlases and describe the methods for their computation. A high-resolution mono-subject template, already validated in the context of DBS (Lalys et al., 2011), along with a multi-subject template (Haegelen et al., 2012), were tested as common spaces. Three motor and five neuro-psychological scores were then used to create anatomo-clinical atlases. The correlation was carried out using a dedicated non-supervised classification system and enabled the extraction of representative clusters to determine the optimum site for therapeutic STN DBS.

2. Materials and Methods

The purpose of this study was to correlate and represent the anatomical position of electrode contacts with clinical outcomes in STN DBS. Firstly, a method for automatic extraction of electrode contacts for each patient was developed. Secondly, an accurate patient images-to-template registration step was studied. Thirdly, the integration of clinical scores from a clinical database was used to extract representative anatomo-clinical clusters, through non-supervised classification.

2.1 Data

The study population consisted of 30 patients (14 women and 16 men, mean age: 60 +/- 5 years) with idiopathic PD who had bilateral STN DBS according to selected inclusion (Langston et al. 1992; Lang and Lozano, 1998; Krack et al., 1998). In particular, one of the inclusion criteria is the improvement of 50% in UPDRS III score during the pre-operative levodopa challenge test. All patients had one pre-operative 3-T T1-weighted MR (Size: 256 x 256 x 182, resolution: 1 mm x 1 mm x 1 mm, Philips Medical Systems) and two CT scans (Size: 203 x 203 x 155, resolution: 0.44 mm x 0.44 mm x 0.6 mm, in post-operative acquisition and 0.5 mm x 0.5 mm x 0.6 mm in pre-operative acquisition, GE Healthcare VCT 64). Pre-operative scans were acquired after attachment to the patient's head of a stereotactic Leksell frame, under local anaesthesia. All images were de-noised using the Non-local means algorithm (Coupe et al., 2008) and

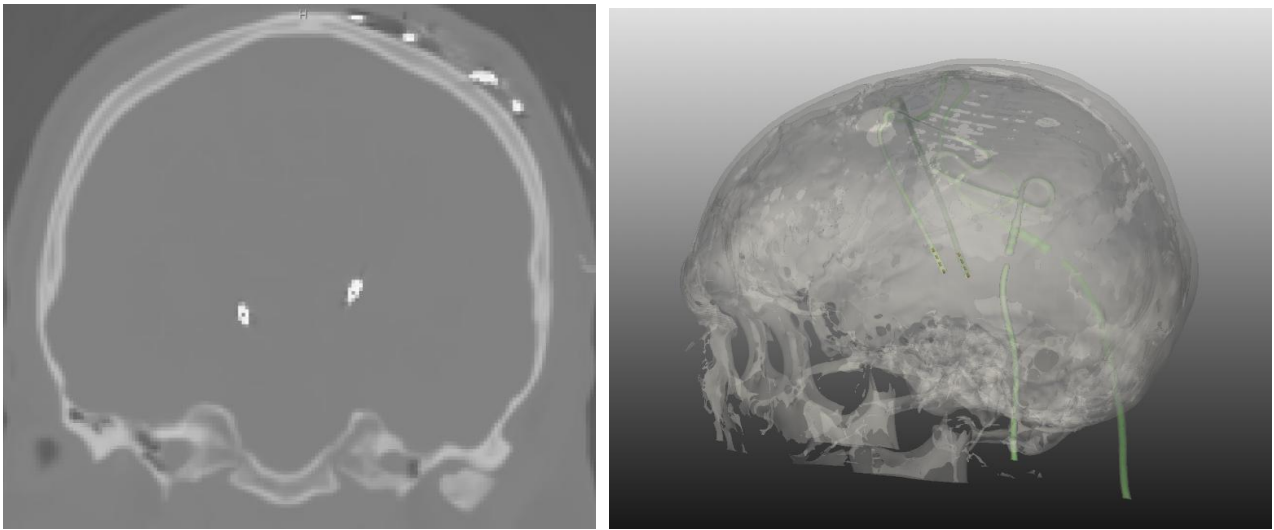
a bias correction algorithm based on intensity values (Mangin, 2000) was also applied to MR images. This study was part of a larger clinical study approved by the local ethical review board.

155 To assess the global patient outcome, we first chose three motor scores: the UPDRS III (Unified Parkinson's Disease Rating Scale, part III) score (Fahn and Elton, 1987), the Schwab & England (Schwab and England, 1968) scale, and the Hoehn & Yahr (Hoehn and Yahr, 1967) scale. For each score, patients were tested without medication (Dopa OFF) immediately prior to surgery (DBS OFF) and three months after it under stimulation (DBS ON), also without medication. We then selected five neuropsychological
160 scores:

- The categorical and the phonemic verbal fluency tests (Troyer et al., 1998) that determine the ease with which patients can produce words.
- The Stroop test (Stroop, 1935) that computes the mental vitality and flexibility
- The Trail Making Test (Reitan, 1958) that determines visual attention and task switching.
- 165 - The Wisconsin Card Sorting Test (Psychological assessment resources, 2003) that estimates the ability to display flexibility in the face of changing schedules of reinforcement.
- The MATTIS score (Mattis, 1988) that tests global cognitive efficiency.

170 **2.2 Contact localization**

For each electrode, the spatial coordinates of the contacts were automatically computed from post-operative CT images by modelling the electrode's axis. We developed a new segmentation technique based on the hypo-signal artefacts (white artefacts) created on CT scans and corresponding to the electrodes. Every CT scan was first simply linearly registered to a reference patient CT. On this reference image, a mask was
175 defined including the two electrodes and entirely excluding the skull. An intensity threshold was applied in order to extract every hypo-signal voxel of both electrodes per patient. Along with a connected component approach for retrieving noise, for each slice, the barycentre of extracted voxels was computed to model the electrodes' axis. By keeping 10 mm from the tip of the electrode, we then performed regression in order to model the area where contacts can finally be obtained by applying geometry constraints of electrode 3389
180 from Medtronic NeuroModulation, USA (Fig. 1.). This automatic procedure was performed for post-operative CT of each patient and gave us all contact locations. It was validated in Mehri et al. (2012) and gave us an error of 0.96 +/- 0.33mm using a linear regression for the modelling of the electrode's axis.



185

Fig. 1. Upper left: Post-operative CT scan of one patient with PD and bilateral STN-DBS. Upper right: Segmentation of the patient's skull, the 2 electrodes and the 8 electrode contacts. Below: Electrode's axis, the 4 extracted contacts and the 4 ground truth contacts for the left side.

190

2.3 Patient to template registration workflow

Patient contacts were warped into a MR template as a common anatomical space for allowing retrospective population statistical analysis. We compared the impact of mono-subject vs. multi-subject MR high-resolution templates on the patient/template non-linear registration accuracy. In opposition to pure histological templates, MR templates are correctly representing the *in vivo* anatomy of the brain. We also compared two non-linear registration methods.

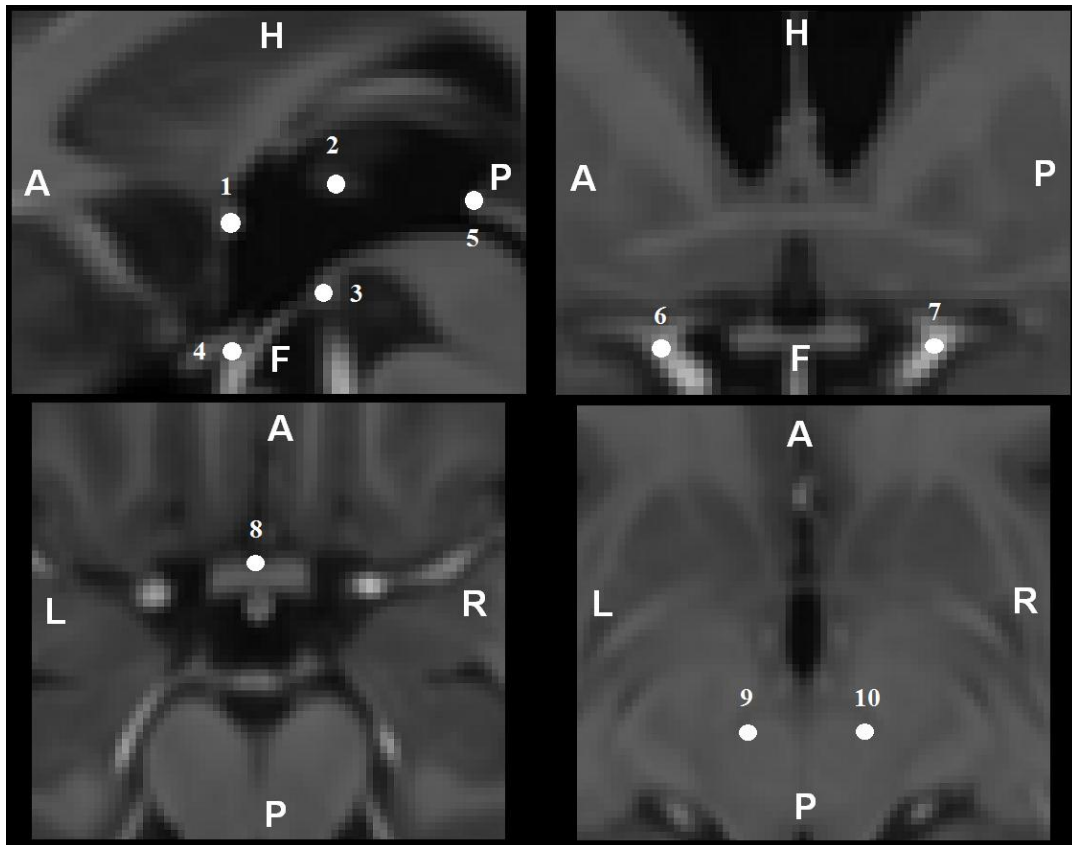
195

The mono-subject template was created from 15 3T MR acquisitions of a healthy 45 year-old male, which were processed and averaged. This high-resolution 3T MRI template (namely the Jannin15), was

200 constructed and assessed by Lalys et al. (2011). The multi-spectral multi-subject, unbiased non-linear average, PD template was made from 57 T1w images of patients with PD (namely the Avg57), thus providing a high-resolution / high signal-to-noise ratio template (Haegelen, 2012). This template allows the specific developmentally important age-ranges and atrophy of PD patients to be taken into account.

The registration workflow was composed of a linear CT to MR patient images registration, a global
205 affine MR-to-template registration, a local affine MR-to-template registration with a mask on deep structures, and a final non-linear registration. Using this procedure the contact positions could be precisely warped into a reference space. We compared the accuracy of two non-linear registration algorithms: the demons approach (www.itk.org) that was used in our previous studies, and the Advanced Normalization ToolS (ANTs) non-linear deformation algorithm used in Symmetric Normalization (SyN) mode that has
210 been shown to be highly effective in the context of MR brain imaging registration (Klein et al., 2009).

For both validation studies, we followed a landmark-based validation approach. Ten anatomical structures were identified within deep-brain structures (Fig. 2.) and manually identified in the images by an expert. Placement of these landmarks on the one hand on the template, and on the other hand on 15 wrapped MR images, allowed us to compute a global registration error. Considering that the intra-subject
215 registration between the CT scan and the MR image was accurate, we only validated the MR-to-template registration. We first compared both templates by keeping the classical linear registration process along with the non-linear Demons algorithm. We then compared, using the best template found, both non-linear registrations (i.e. Demons Vs ANTs-SyN) using a student t-test.



220

Fig. 2. Anatomical landmarks used for the validation study

1 - Anterior Commissure

2 - Interthalamic adhesion on the middle of the axial slice

225

3 - Posterior Commissure

4 - Infundibular recesses

5 - Middle of the mammillary bodies

6,7 - Left and right internal carotid division into anterior and middle cerebral arteries

8 - Center of the anterior portion of the optic chiasma

230

9,10 - Centers of the left and right red nuclei

2.4 Anatomico-clinical atlases

235

For all scores and for representing the degree of improvement or worsening of the patient, the difference between DBS ON and DBS OFF values was computed. In order to represent all improvement or worsening of patients on a similar scale, all clinical scores were statistically normalized. On each score, we subtracted the mean and divided by the variance of the dedicated score. After normalization, the data closely followed a normal distribution (with mean=0 and standard deviation=1) and were more easily usable for data variation comparisons.

240

For each score, an atlas was computed as the list of active contact coordinates from all patients associated with the corresponding difference value. The active contacts were those at three months post-surgery. 3D visualization consisted in displaying the list of points represented with a colour code related to the patient clinical scores. Each clinical score can therefore create one anatomo-clinical atlas. Due to random errors or missing values in reporting scores, the initial clinical score dataset of 30 patients dropped to 23 for the motor analysis, but remained at 30 for the neuropsychological analysis.

2.5 Non-supervised classification

After atlas construction, we performed a segmentation step using non-supervised techniques. Hierarchical Ascendant Classification (HAC) was used on clinical scores merged with coordinates to search homogeneous groups of patients and extract general clinical trends. Feature vectors were composed of four features: the value of the x-axis, y-axis, z-axis and the score difference value. HAC operates by successively merging pairs of existing clusters, where the next pair of clusters to be merged is chosen as the pair with the smallest distance. This linkage between clusters a and b was performed using the Ward criterion along with the weighted Euclidean distance:

$$d^2(a,b) = n_a n_b \frac{\sum_{k=1}^M w_k |\bar{x}_{ak} - \bar{x}_{bk}|}{n_a + n_b}$$

where $\bar{x}_a = \frac{1}{n_a} \sum_{i=1}^{n_a} x_{ai}$ is the centroid of cluster a (resp. b), n_a (resp. n_b) is the number of objects in cluster

a (resp. b), and w_k are the weights, specified by $w_1 = w_2 = w_3 = \frac{1}{12}$ and $w_4 = \frac{3}{4}$. The dendrogram was cut in order to obtain two or three clusters for each clinical score. Validation of the non-supervised classification was performed with an ANOVA test.

3. Results

270

The registration error was computed for the different combinations of non-linear registrations and templates. First, results of Table. 1. show that the new multi-subject template was significantly better than the mono-subject one (p-value = 0.025).

	Mean registration error (mm)	Std deviation (mm)	Test student
Jannin15 template + Demons non-linear registration	1,23	0,12	p-value = 0,025
Avg57 template + Demons non-linear registration	1,15	0,09	

275

Table. 1. Landmark-based validation for the comparison of the Jannin15 vs. Avg57 templates on patient to atlas non-linear registration using Demon's method.

Table. 2. then shows that the new non-linear registration method (ANTs-SyN) gave best results compared to the Demons algorithm (p-value = 0.05). For the rest of the study, the two new parameters were then conserved, providing a global registration error of 0.98 +/- 0.17mm. Patient's contacts were also warped in the Talairach space for clinical verification. The origin of the electrode contact coordinates was the midpoint between the AC and the PC points. Three months after surgery, the mean position of the active electrode's contacts for the left electrodes was X=+14.33 mm for the lateral direction, Y=-1.79 mm for antero-posterior direction, Z=-1.01 mm for the dorso-caudal direction, and X=-14.65 mm, Y=-1.88 mm, Z=-0.77 mm for the right electrodes. The stimulation parameters used were frequency at 130 Hz, pulse duration for 60 microseconds for all the patients and a mean voltage of $2,14 \pm 0,34$ V.

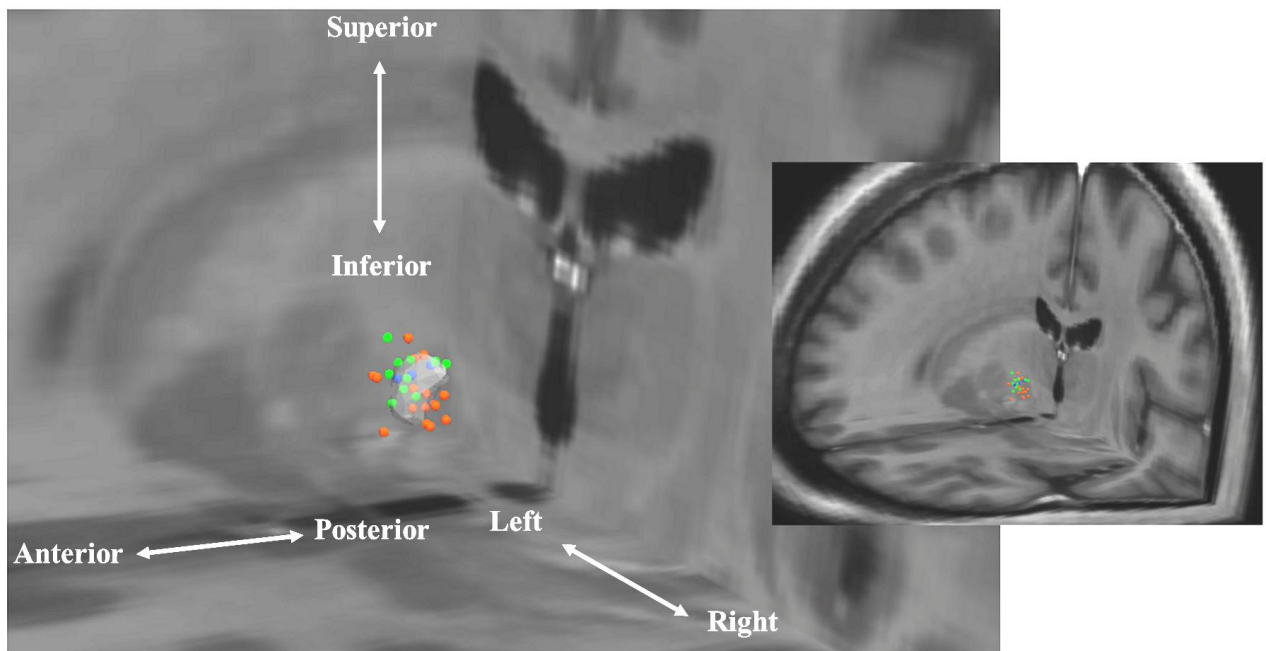
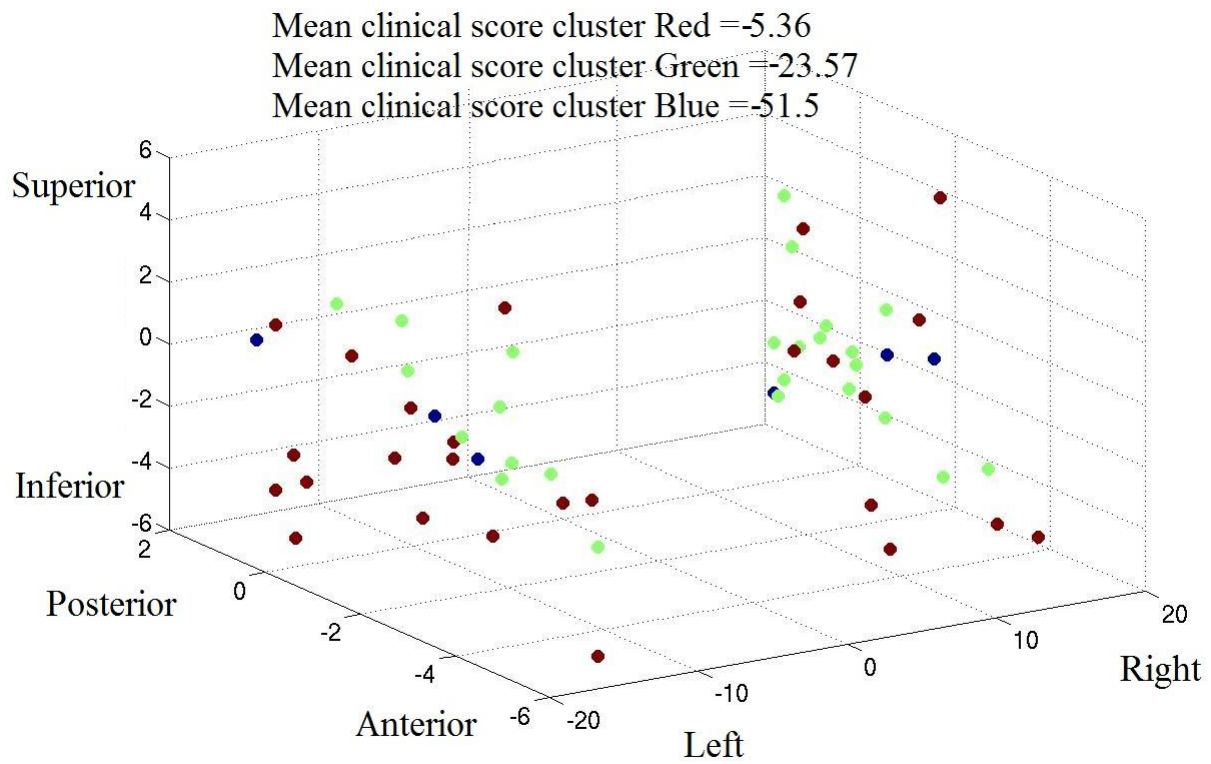
285

	Mean registration error (mm)	Std deviation (mm)	Test student
Avg57 template + Demons non-linear registration	1,15	0,09	p-value = 0,05
Avg57 template + ANTS-SyN non-linear registration	0,98	0,17	

290 **Table. 2.** Landmark-based validation for the comparison of the Demons vs. ANTS-SyN non-linear registration methods.

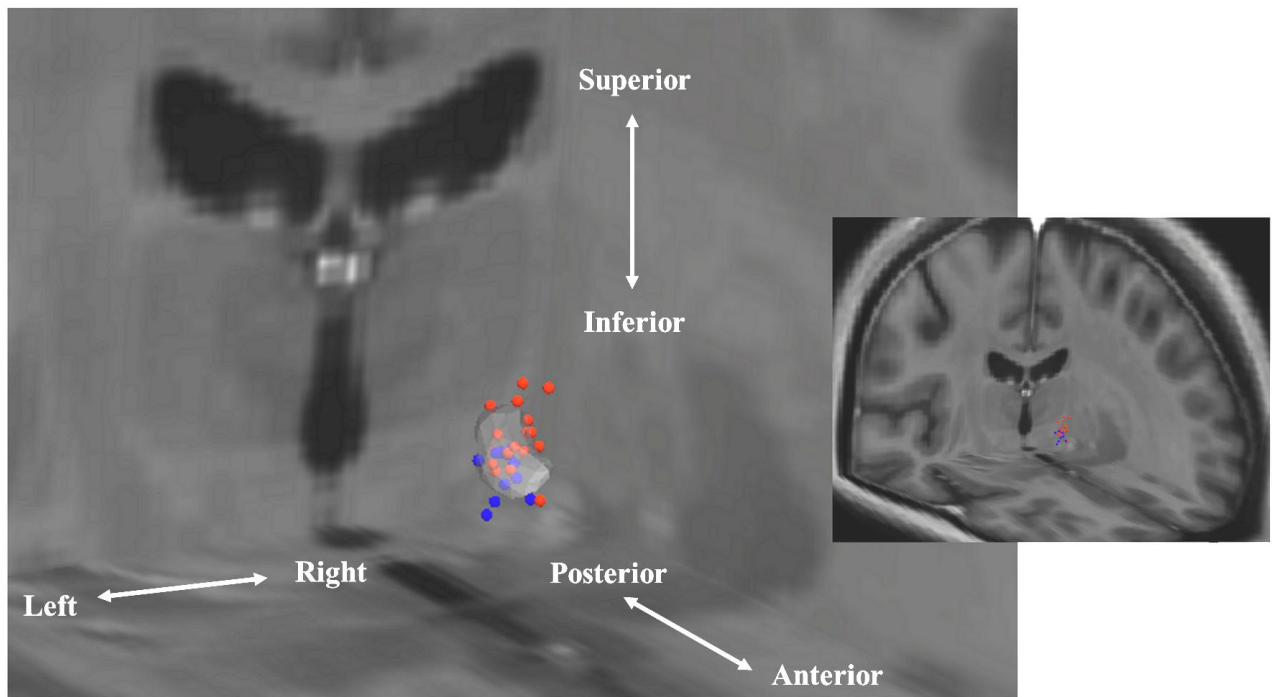
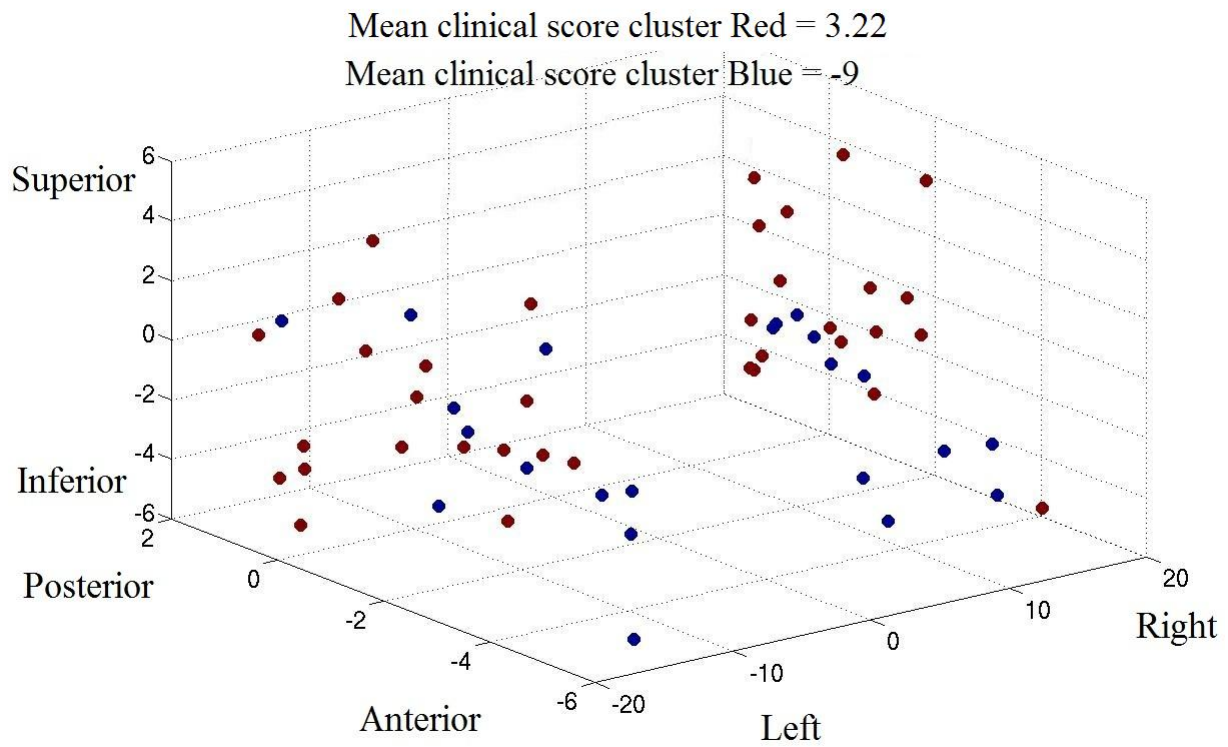
For all following figures, we represent the results in the Talairach space as well as in Avg57 template to improve clinical representation and interpretation. For each clinical score, clustering was performed for both hemispheres independently. For each clinical score, we noticed that the group of patients (clusters) that were extracted for both hemispheres were identical. The x-axis represents the left-right direction, the y-axis represents the antero-posterior direction, and the z-axis represents the caudo-cranial direction. The scale of figures is shown in mm. Fig. 3. shows a greater improvement of UPDRS III for cluster Blue compared to clusters Red and Green ($p = 10^{-6}$). Majority of the contacts of the cluster Blue were in the postero-superior region of the STN. Hoehn & Yahr and Schwab & England scores showed similar results, but with a fuzzy definition of clusters ($p = 5.10^{-2}$).

Fig. 4. shows a deterioration of the categorical fluency in the posterior region (cluster Red), and an improvement in the antero region (cluster Blue) ($p = 10^{-4}$). For the phonemic fluency we found a general deterioration for all patients, without apparent separation of clusters. STROOP score analysis (Fig. 5.) indicated score improvement in the postero-superior region (cluster Red), and deterioration in the antero-inferior region ($p = 10^{-5}$) (cluster Blue). For the three other neuropsychological scores (Trail Making Test, Wisconsin Card Sorting Test, MATTIS score), no significant clusters were found ($p > 5.10^{-2}$). Table. 3. summarizes results of the analysis using the different clinical scores.



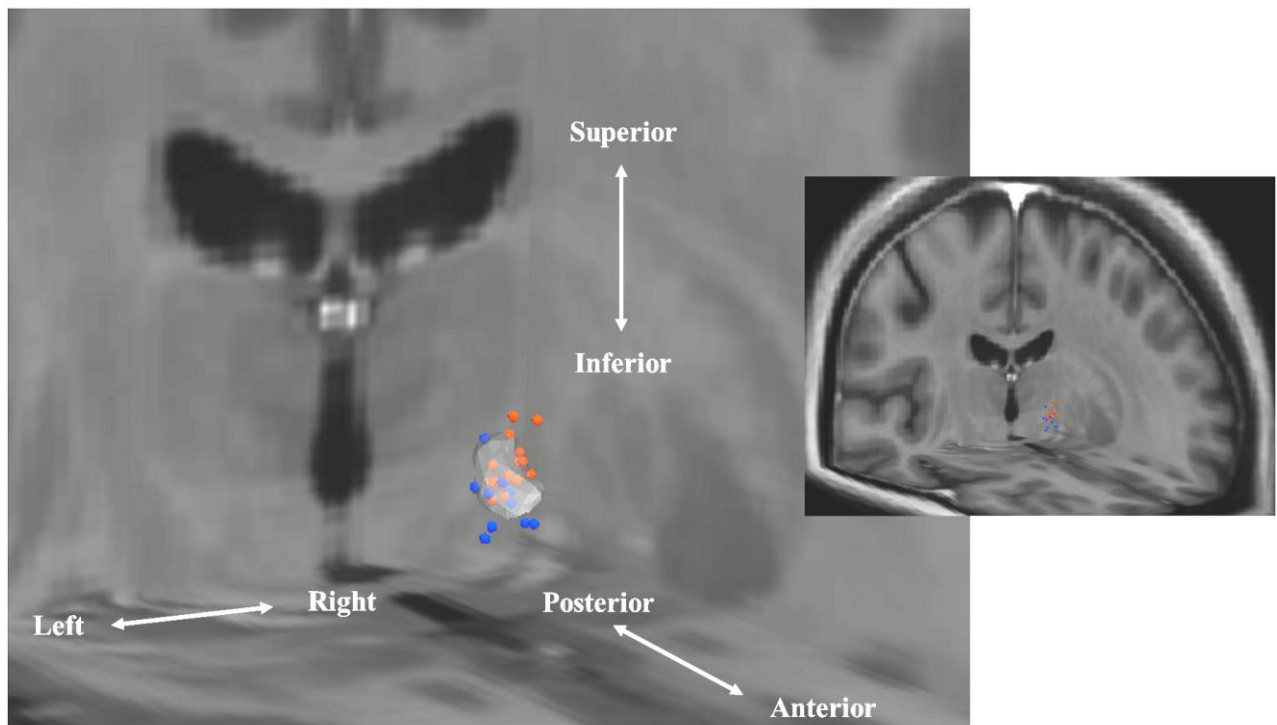
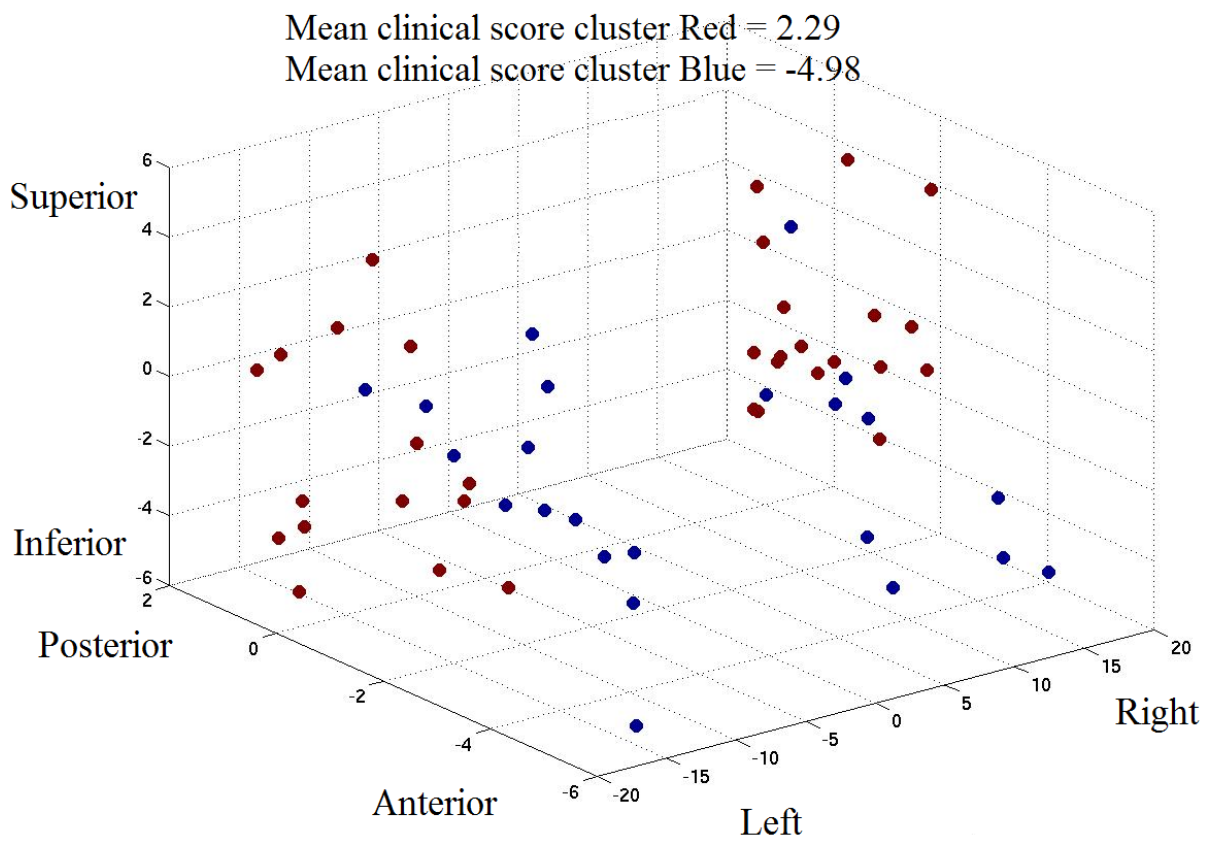
310

Fig. 3. UPDRS III analysis, with the cluster display in Talairach coordinates (above), and the cluster display in the template space for the left hemisphere with the STN (below).



315

Fig. 4. Categorical fluency analysis, with the cluster display in Talairach coordinates (above), and the cluster display in the template space for the right hemisphere with the STN (below).



320

Fig. 5. STROOP analysis, with the cluster display in Talairach coordinates (above), and the cluster display in the template space for the right hemisphere with the STN (below).

Clinical scores	Cluster	Number of patients	Mean clinical score (Post-pre-op)	Clinical signification	Major STN zone of stimulation
UPDRS III	<i>Cluster Blue</i>	3	-51.5	Very good improvement	Postero-superior region
	<i>Cluster Green</i>	11	-23.6	Good improvement	Superior and Posterior regions
	<i>Cluster Red</i>	15	-5.4	Stabilisation	Anterior and inferior regions
Categorical fluency	<i>Cluster Blue</i>	11	-9	Improvement	Antero region
	<i>Cluster Red</i>	18	3.2	Deterioration	Posterior region
STROOP	<i>Cluster Blue</i>	13	-5	Deterioration	Antero-inferior region
	<i>Cluster Red</i>	15	2.6	Improvement	Postero-superior region
Others	<i>No significant clusters found</i>				

325

Table 3. Summarization of clusters found for each clinical score, i.e. the number of patients per cluster, the dedicated mean clinical score, the clinical signification of the mean clinical score and the major STN zone of stimulation of the patients belonging to this cluster.

330

4. Discussion

This article reports about the construction of anatomo-clinical atlases in patients with STN stimulation and severe disabled Parkinson's disease. To our knowledge, we reported for the first time a discrepancy between a very good motor improvement by targeting the postero-superior region of the STN and an inevitable deterioration of the categorical and phonemic fluency in the same region. These results were provided by the use of tools already validated but never used together to provide the association of clinical scores with electrode contacts within a normalized space in the context of STN DBS.

340

4.1 Contact localization and representation

Many publications advocate the use of post-operative MRI to determine the electrode's contact coordinates (Saint-Cyr et al., 2002; Pollo et al., 2007) despite the possible adverse effects related to MRI acquisition with implanted DBS electrodes (Medtronic, 2006). The use of MRI has recently been validated by Lee et al.

(2010) with a study showing that there were no significant discrepancies between the centres of electrodes
345 estimated by CT and MRI. In this project, the spatial coordinates of the 4 contacts per electrode were
automatically computed from post-operative CT images. The automatic contact localization algorithm gave
us satisfactory results with an average error of 0.96 +/- 0.33mm (Mehri et al., 2012). This error, even quite
low, has to be taken into account in the final cluster analysis. Considering the relative small size of the STN
and its sub-regions, this bias will still have to be minimized using more robust automatic segmentation
350 algorithms.

Comparison of electrode positions of STN DBS estimated in the immediate post-operative CT with
those estimated 6 months after surgery showed that they may contain some discrepancies (Kim et al., 2010).
Results also indicated that it is often due to the extensive pneumocephalus. Ideally, this bias could be
reduced by comparing clinical scores evaluated 6 months after the surgery with a post-operative CT
355 acquired within the same period.

We modelled the signal by a point corresponding to the centre of the artefact. For further developments,
it will be crucial to integrate the influence of stimulation on the surrounding biological tissues. Some
studies on the modelling of tissues and electrical influence of electrodes in the context of DBS have
recently been published (Buston et al., 2011). Complete DBS modelling would integrate all of these data to
360 provide the highest possible precision.

4.2 Template and registration workflow

We compared the impact of mono-subject vs. multi-subject MR high-resolution templates on the
patient/atlas non-linear registration accuracy. Both templates allowed the production of reference images
365 with a high degree of anatomical detail, both for deep-brain structures and for the cerebral cortex. The
accuracy of the patient images-to-template registration is an important step, which may considerably impact
the quality of the findings. In DBS, major sources of errors are due to the identification of basal ganglia
from patient-specific images. Therefore, during the procedure, we added a local registration involving
targeted structure (STN), intended to improve basal ganglia registration. Results of the template-to-patient
370 registration comparison have shown that the new multi-subject template increases the accuracy of a patient-
to-template basal ganglia registration. This is explained by the fact that the single subject template did not

take into account brain atrophy of the patient population. The impact of this new template was significant and it has improved not only registration quality (0.98mm) but also retrospective visualization. During the registration workflow, intra-subject rigid registration appears to be very effective, especially when native
375 acquisitions are subject to a step of reliable pre-processing as we performed in our registration procedure. On the contrary, the patient-to-template registration procedure, including linear and non-linear registrations steps, was subject to small errors that can explained this registration error of 0.98mm. Similarly to the localization of the electrode contacts, this bias has to be taken into account when analysing the final cluster results.

380 Many active contacts are located outside the STN within atlases. This can be partially explained by the error induced during the warping step, though other explanations could be put forward. First, the electrical stimulation zone is in fact larger than the simple contact position, recovering a region wide enough to accept a targeting uncertainty. It is known, in any case, that the field of stimulation can have a spread of up to 2 mm within the brain (Buston et al., 2011). Secondly, deep-brain tissues and nerves are deeply
385 interconnected and nerves at the periphery of structures have an influence on the structure itself.

The coordinates of the stimulated contacts were more lateral than those previously reported (Krack et al., 2003; Dujardin et al., 2004; Houeto et al., 2002). One explanation could be that the targeting in our study was based on 3T MRI and not on ventriculography as in other centres. The visualisation of the STN on T2 pre-operative MRI allowed direct targeting instead of probabilistic targeting based on the Talairach atlas.
390 The neurosurgeons attempted to place the electrode in the postero-superior part of the STN as they knew that it is involved in motor component of the STN (Rodriguez-Oro et al., 2001; Theodosopoulos et al., 2003).

395 **4.3 Clinical scores**

Each clinical score was used to extract representative clusters. Compared to clustering on clinical scores only, adding coordinates allows a better definition of clusters and a better understanding of DBS efficiency according to contact locations. Motor and neuropsychological scores were analysed to assess the patient outcome (Benabid et al., 2000; Brontë-Stewart et al., 2010). Other teams have also focused on the analysis
400 of clinical scores in the context of STN DBS (Guehl et al., 2007; Lamotte et al., 2002).

In our procedure, the main issue was the inability to separate the response to DBS stimulation of the

right and left contacts. Each test was performed with both activated contacts. Separate evaluations would involve many hours without medication and stimulation in order to lose previous therapeutic and stimulation effects. In the pre-operative targeting procedure, surgeons first localized the optimum target position of one side, and the target position of the other side was automatically computed from the definition of the mid-sagittal line. These targets were used as an initial position that had to be refined per-operatively.

Other variables that could have been taken into account are the different contact parameters, i.e. the frequency, pulse duration and voltage. From the 30 patients in our study, these parameters did not differ among patients, so we did not include the stimulation parameters in the study. Moreover, the standard deviation of the stimulation voltage was low and not sufficiently discriminant to be included.

Because of their low granularity, values of the Schwab & England and Hoehn & Yahr scales turned out to be less representative than UPDRS III. Moreover, our method was more useful for quantitative continuous data than for quantitative discontinuous data. For this reason, even though the results of motor scores studies were almost identical, the visualization of the atlas containing the UPDRS III provides more information. Using these clinical data, the postero-superior region has been found to be the most effective region for motor improvement. This follows conclusions of previously published work on the topic (Guehl et al., 2007; Lamotte et al., 2002), and can be explained by the fact that this part of the STN (usually named the dorso-lateral part) is involved in sensory and motor functions (Maks et al., 2009). Indeed, as shown in the introduction, a subdivision of the STN into a ventromedial associative and a medial limbic (psychology, mood) territories is described in the literature. Recent studies (Karachi et al., 2005; Lambert et al., 2012), stated that the motor region was situated in the posterior portion of the nucleus. Our results related to motor improvements therefore support this hypothesis. Moreover, this subdivision can explain that the antero-inferior (corresponding to the limbic territory) region has shown significant neuropsychological side effects such as the deterioration of the Stroop score. In Lambert et al., (2012), the limbic zone was found to be in the anterior portion of the STN. Results on the Stroop score are also quite satisfactory as it can be explained by recent discoveries on STN territories. Lastly, our study highlighted at our knowledge for the first time, that the categorical fluency was improved in the anterior region of the STN, whereas the categorical fluency was worse in its postero-superior region. Moreover, the phonemic fluency was worse after STN stimulation

430 whatever the region of the STN stimulated. This last result was not surprising as the deterioration of
phonemic verbal fluency is one of the most observed side effects in STN DBS, though the phenomenon is
not really understood (Temel et al., 2006; Saint-Cyr et al., 2000). The deterioration of the phonemic fluency
seems to be impossible to avoid after STN stimulation and the categorical fluency only improved in the
anterior region that is not the best region in terms of motor improvement. We can imagine multiple sub-
435 regions within the STN where the stimulation may involve these side effects, but the extraction of finer
spatial clusters would require a larger study population. Our results could also demonstrate that the STN is
not so well subdivided into three different functional territories but the motor, associative and limbic
territories are more probably mixed due to diffused interneuron's connection.

Lastly, concerning all other neuropsychological scores (Trail Making Test, Wisconsin Card Sorting Test,
440 MATTIS score), no clusters were clearly defined, resulting in small statistical differences. With our current
data, no statistical clusters could be extracted from these scores yet, either because of the number of patients
associated with the different bias of the analysis, or because no significant effects were observed amongst
patients for these specific clinical scores.

445 **5. Conclusion**

In this paper, we focused on identifying optimum sites for STN DBS by studying symptomatic motor
improvement along with neuropsychological side effects. The underlying mechanisms of action of DBS
surgery have not yet been identified. The concept of anatomico-clinical atlases, introduced in this paper,
450 allows the integration, within a single coordinate system, of a digitized brain MRI template, previous target
coordinates of implantations, and various clinical scores. Each clinical score produced one anatomico-clinical
atlas, associating the degree of improvement or worsening of the patient with its active contacts.
Additionally, non-supervised classification was performed on scores and coordinates to extract clusters for
determining optimum electrode contact coordinates. We showed how to extract knowledge gained from
455 population data based on the correlation between anatomical location of contacts and clinical data. To our
knowledge, we reported for the first time a discrepancy between a very good motor improvement by
targeting the postero-superior region of the STN and an inevitable deterioration of the categorical and
phonemic fluency in the same region. The proposed anatomico-clinical atlases were created to provide the

surgeons with additional assistance for better understanding of DBS-related phenomena. It could find its
460 application in pre-operative planning (Dawant et al., 2007; Stancanello et al., 2008) as well as for post-
operative assessment (Lalys et al., 2009). As targeting is mainly based on the surgeon's knowledge and
experience, it could serve as an additional source of information obtained from retrospective studies for
reducing time and predicting motor outcome and possible post-operative adverse-effects. The underlying
challenge would be to reduce the intra-operative time required for electrode contact adjustment by
465 microelectrode recordings. The actual local anaesthesia would be replaced by a general anaesthesia, which
would completely alter the surgical routine by reducing surgical staff workload, improving patient care and
increasing medical safety. Alternatively, such atlases also provide an understanding of previous
interventions that didn't give satisfactory results. In such cases, active contacts of a new patient can be
warped into the common space, displayed for post-operative assessment, and inserted into a new analysis
470 for updating the atlases. This work yields many flourishing studies in the field, including further clinical
data such as quality of life or cognitive criteria.

Acknowledgments. The authors would like to acknowledge Alexandre Bonnet for his contribution to the
registration validation studies, Dr Eduardo Pasqualini, Vladimir Fonov. The authors would like to thank the
475 French Research Agency (ANR) for funding this study through the ACouStiC project.

References

- 480 Aubert-Broche B, Evans AC, Collins L. A new improved version of the realistic digital brain phantom. *NeuroImage*, 2006; 32: 138-45.
- Bardinet E, Bhattacharjee M, Dormont D, Pidoux B, Malandain G, Schüpbach M, Ayache N, Cornu P, Agid Y, Yelnik J. A three-dimensional histological atlas of the human basal ganglia. II. Atlas deformation strategy and evaluation in deep brain stimulation for Parkinson disease. *J Neurosurg*, 2009; 110: 208-19.
- 485 Benabid AL, Krack P, Benazzouz A, Limousin P, Koudsie A, Pollak P. Deep brain stimulation of the subthalamic nucleus for Parkinson's disease: methodologic aspects and clinical criteria. *Neurology*, 2000 ; 55 : 40-4.
- Benabid AL, Koudsié A, Benazzouz A, Fraix V, Ashraf A, Le Bas JF, Chabardes S, Pollak P. Subthalamic stimulation for Parkinson's disease. *Arch Med Res*, 2000; 31: 282-9.
- Biseul I, Sauleau P, Haegelen C, Trebon P, Drapier D, Raoul S, Drapier S, Lallement F, Rivier I, Lajat Y, Verin M.
- 490 Fear recognition is impaired by subthalamic nucleus stimulation in Parkinson's disease. *Neuropsychologia*, 2005; 43: 1054-9.
- Burrows AM, Ravin PD, Novak P, Peters ML, Dessureau B, Swearer J, Pilitsis JG. Limbic and motor function comparison of deep brain stimulation of the zona incerta and subthalamic nucleus. *Neurosurgery*, 2011; 70(1): 125-30.
- 495 Buston CR, Cooper SE, Henderson JM, Wolgamuth B, McIntyre CC. Probabilistic analysis of activation volumes generated during deep brain stimulation. *NeuroImage*, 2011; 54(3): 2096-104.
- Brontë-Stewart H, Louie S, Batya S, Henderson JM. Clinical motor outcome of bilateral subthalamic nucleus deep-brain stimulation for Parkinson's disease using image-guided frameless stereotaxy. *Neurosurgery*, 2010; 67(4): 1088-93.
- 500 Brücke C, Kupsch A, Schneider GH, Hariz MI, Nuttin B, Kopp U, Kempf F, Trottenberg T, Doyle L, Chen CC, Yarrow K, Brown P, Kühn AA. The subthalamic region is activated during valence-related emotional processing in patients with Parkinson's disease. *Eur J Neurosci*, 2007; 26: 767-74.
- Chakravarty M, Bertrand G, Hodge CP, Sadikot AF, Collins DL. The creation of a brain atlas for image guided neurosurgery using serial histological data. *NeuroImage*, 2006; 30(2): 359-76.
- 505 Coupe P, Yger P, Prima S, Hellier P, Kervrann C, Barillot C. An optimized blockwise non local means denoising filter for 3D magnetic resonance images. *IEEE TMI*, 2008; 24(4): 425-41.

- Dawant B, D'Haese PF, Pallavaram S, Li R, Yu H, Spooner J, Davis T, Kao C, Konrad P. The VU- DBS project: integrated and computer-assisted planning, intra-operative placement, and post-operative programming of deep-brain stimulators. *SPIE Medical Imaging*, 2007; 6509(1): 650907.
- 510 D'Haese PF, Cetinkaya E, Konrad PE, Kao C, Dawant BM. Computer-aided placement of deep brain stimulators: From planning to intraoperative. *IEEE TMI*, 2005; 24(11): 1469-78.
- D'Haese PF, Pallavaran S, Yu H, Spooner J, Konrad PE, Dawant BM. Deformable physiological atlas-based programming of deep brain stimulators: a feasibility study. *WBIR*, Utrecht, The Netherlands, 2006; 144-50.
- D'Haese PF, Pallavaram S, Li R, Remple MS, Kao C, Neimat JS, Konrad PE, Dawant BM. CranialVault and its
515 CRAVE tools: A clinical computer assistance system for deep brain stimulation (DBS) therapy. *Med Image Anal*, 2010; 16(3): 744-53.
- Dormont D, Seidenwurm D, Galanaud D, Cornu P, Yelnik J, Bardinet E. Neuroimaging and deep brain stimulation. *AJNR*, 2010; 31(1): 15-23.
- Dujardin K., Blairy S, Defebvre L, Krystkowiak P, Hess U, Blond S, Destee A. Subthalamic nucleus stimulation
520 induces deficits in decoding emotional facial expressions in Parkinson's disease. *J Neurol Neurosurg Psychiatry*, 2004; 75: 202-8.
- Fahn Y, Elton R. Unified Parkinson's disease rating scale. In Fahn S, Marsden C, Calne D, Goldstein M (eds): *Recent Developments in Parkinson's Disease*, 2, Florham Park, NJ: Macmillan, 1987; 153-63.
- Finnis KW, Starreveld YP, Parrent AG, Sadikot AF, Peters TM. Three-dimensional database of subcortical
525 electrophysiology for image-guided stereotactic functional neurosurgery. *IEEE Trans Med Imaging*, 2003; 22(1): 93-104.
- Fonov V, Evans AC, Botteron K, Almli CR, McKinstry RC, Collins DL. Unbiased average age-appropriate atlases for pediatric studies. *NeuroImage*, 2011; 54: 313-27.
- Greenhouse I, Gould S, Houser M, Hicks G, Gross J, Aron AR. Stimulation at dorsal and ventral electrode contacts
530 targeted at the subthalamic nucleus has different effects on motor and emotion functions in Parkinson's disease. *Neuropsychologia*, 2011; 49: 528-34.
- Guehl D, Edwards R, Cuny E, Burbaud P, Rougier A, Modolo J, Beuter A. Statistical determination of the optimal subthalamic nucleus stimulation site in patients with Parkinson disease. *J Neurosurgery*, 2007; 106: 101-10.
- Guo T, Finnis KW, Parrent AG, Peters TM. Visualization and navigation system development and application for
535 stereotactic deep-brain neurosurgeries. *Comput Aided Surg*, 2006; 11: 231-9.
- Haegelen C, Coupe P, Fonov V, Guizard N, Jannin P, Morandi X, Collins DL. Automated segmentation of basal ganglia and deep brain structures in MRI of Parkinson's Disease. *Int J Comput Assist Radiol Surg*, 2012 (In press)

- Hamani C, Saint-Cyr JA, Fraser J, Kaplitt M, Lozano AM. The subthalamic nucleus in the context of movement disorders. *Brain*, 2003; 127(1): 4-20.
- 540 Hoehn M, Yahr M. Parkinsonism: onset, progression and mortality. *Neurology*, 1967; 17(5): 427-42.
- Houeto JL, Mesnage V, Mallet L, Pillon B, Gargiulo M, du Moncel ST, Bonnet AM, Pidoux B, Dormont D, Cornu P, Agid Y. Behavioural disorders, Parkinson's disease and subthalamic stimulation. *J Neurol Neurosurg Psychiatry*, 2002; 72: 701-7.
- Huebl J, Schoenecker T, Siegert S, Brücke C, Schneider GH, Kupsch A, Yarrow K, Kühn AA. Modulation of
545 subthalamic alpha activity to emotional stimuli correlates with depressive symptoms in Parkinson's disease. *Movement disorders: official journal of the Movement Disorder Society*, 2011; 26: 477-83.
- Karachi C, Yelnik J, Tandé D, Tremblay L, Hirsch E, François C. The pallidum-subthalamic projection: An anatomical substrate for nonmotor functions of the subthalamic nucleus in primates. *Mov Disord*, 2005; 20(2): 172-80.
- Khan MF, Mewes K., Gross RE, Skrinjar O. Assessment of brain shift related to deep brain stimulation surgery.
550 *Stereotact Funct Neurosurg*, 2008; 86(1): 44-53.
- Kim YH, Kim HJ, Kim C, Kim DG, Jeon BS, Paek SH. Comparison of electrode location between immediate postoperative day and 6 months after bilateral subthalamic nucleus deep brain stimulation. *Acta Neurochirurgica*, 2010; 152(12): 2037-45.
- Klein A, Andersson J, Ardekani BA, Ashburner J, Avants B, Chiang MC, Christensen GE, Collins DL, Gee J, Hellier
555 P, Song JH, Jenkinson M, Lepage C, Ruekert D, Thompson P, Vercauteren T, Woods RP, Mann JJ, Parsey RV. Evaluation of 14 nonlinear deformation algorithms applied to human brain MRI registration. *NeuroImage*, 2009; 46(3): 786-802.
- Krack P, Pollak P, Limousin P, Hoffmann D, Xie J, Benazzouz A, Benabid AL. Subthalamic nucleus or internal pallidal stimulation in Young onset Parkinson's disease. *Brain*, 1998; 121: 451-7.
- 560 Krack P, Batir A, Van Blercom N, Chabardes S, Fraix V, Ardouin C, Koudsie A, Limousin PD, Benazzouz A, Le Bas JF, Benabid AL, Pollak P. Five-year follow-up of bilateral stimulation of the subthalamic nucleus in advanced Parkinson's disease. *N Engl J Med*, 2003; 349: 1925-34.
- Kühn AA, Hariz MI, Silberstein P, Tisch S, Kupsch A, Schneider GH, Limousin-Dowsey P, Yarrow K, Brown P. Activation of the subthalamic region during emotional processing in Parkinson disease. *Neurology*, 2005; 65: 707-
565 13.
- Lalys F, Haegelen C, Abadie A, Jannin P. Post-operative assessment in Deep Brain Stimulation based on multimodal images: registration workflow and validation. In *Medical Imaging 2009: Visualization, Image-Guided Procedures, and Modelling*, 2009.

- Lalys F, Haegelen C, Ferre JC, El-Ganaoui O, Jannin P. Construction and assessment of a 3T MRI brain template. *NeuroImage*, 2011; 49(1): 345-54.
- 570 Lambert C, Zrinzo L, Nagy Z, Lutt, A, Hariz M, Foltynie T, Draganski B, Ashburner J, Frackowiak R. Confirmation of functional zones within the human subthalamic nucleus: Patterns of connectivity and sub-parcellation using diffusion weighted imaging. *NeuroImage*, 2012; 60(1): 83-94.
- Lang AE, Lozano AM. Parkinson's Disease. *The New England Journal of Medicine*, 1998; 339(15): 1044-53.
- 575 Langston JW, Widner H, Goetz CG, Brooks D, Fahn S, Freeman T, Watts R. Core assessment program for intracerebral transplantation (CAPIT). *Mov Dis*, 1992; 7(1): 2-13.
- Lanotte MM, Rizzone M, Bergamasco B, Faccani G, Melcarne A, Lopiano L. Deep Brain Stimulation of the subthalamic nucleus: anatomical, neurophysiological, and outcome correlations with the effects of stimulation. *J Neurol Neurosurg Psychiatry*, 2002; 72: 53-8.
- 580 Lee JY, Kim JW, Lee JY, Lim YH, Kim C, Kim DG, Jeon BS, Paek SH. Is MRI a reliable tool to locate the electrode after deep brain stimulation surgery? Comparison study of CT and MRI for the localization of electrodes after DBS. *Acta Neurochir*, 2010; 152(12): 2029-36.
- Lenglet C, Abosch A, Yacoub E, De Martino F, Sapiro S, Hare, N. Comprehensive in vivo Mapping of the Human Basal Ganglia and Thalamic Connectome in Individuals using 7T MRI. *PLOS*, 2012; 7(1).
- 585 Lhommée E, Klinger H, Thobois S, Schmitt E, Ardouin C, Bichon A, Kistner A, Fraix V, Xie J, Aya Kombo M, Chabardès S, Seigneuret E, Benabib AL, Mertens P, Polo G, Carnicella S, Quesada JL, Bosson JL, Broussolle E, Pollak P, Krack P. Subthalamic stimulation in Parkinson's disease: restoring the balance of motivated behaviours. *Brain, a journal of neurology*, 2012; 135: 1463-77.
- Maks CB, Butson CR, Walter BL, Vitek JL, McIntyre CC. Deep brain stimulation activation volumes and their association with neurophysiological mapping and therapeutic outcomes. *Journal of Neurology Neurosurgery and Psychiatry*, 2009; 80(6): 659-66.
- 590 Mallet L, Schüpbach M, N'Diaye K, Rémy P, Bardinet E, Czernecki V, Welter ML, Pelissolo A, Ruberg M, Agid Y, Yelnik J. Stimulation of subterritories of the subthalamic nucleus reveals its role in the integration of the emotional and motor aspects of behavior. *Proceedings of the National Academy of Sciences of the United States of America*, 2007; 104: 10661-6.
- 595 Mangin JF. Entropy minimization for automatic correction of intensity non uniformity. Hilton Head Island, S. IEEE Press, 2000; 162-9.
- Mattis S. Dementia Rating Scale. Professional Manual. Odessa, FL: Psychological Assessment resources, 1988.
- Medtronic. MRI guidelines for medtronic deep brain stimulation systems, 2006.

- 600 Mehri M, Lalys F, Maumet C, Haegelen C, Jannin P. Analysis of electrodes placement and deformations in deep brain stimulation. *SPIE Medical Imaging*. 2012; 8316-8332.
- Nowinski WL, Belov D, Benabid AL. An algorithm for rapid calculation of a probabilistic functional atlas of subcortical structures from electrophysiological data collected during functional neurosurgery procedures. *NeuroImage*, 2003; 18: 143-55.
- 605 Nowinski WL, Belov D, Pollak P, Banabid AL. Statistical analysis of 168 bilateral subthalamic nucleus implantations by means of the probabilistic functional atlas. *Neurosurgery*, 2005; 57(4): 319-30.
- Nowinski WL, Thirunavuukarasuu A, Liu J, Benabid AL. Correlation between the anatomical and functional human subthalamic nucleus. *Stereotact Funct Neurosurg*, 2007, 85: 88-93.
- Pallavaram S, Dawant BM, Remple M, Neimat JS, Kao C, Konrad PE, D'Haese, PF. Effect of brain shift on the
610 creation of functional atlases for deep brain stimulation surgery. *Int J Comp Assist Radiol Surg*, 2009; 5(3): 221-8.
- Pallavaram S, D'Haese PF, Kao C, Yu H, Remple M, Neimat JS, Konrad PE, Dawant BM. A new method for creating electrophysiological maps for DBS surgery and their application to surgical guidance. *Med Imma Comput Comput Assist Interv*, 2008; 670-7.
- Parsons TD, Rogers SA, Braayen AJ, Woods SP, Troster AI. Cognitive sequelae of subthalamic nucleus deep brain
615 stimulation in Parkinson's disease: a meta-analysis. *Lancet Neurol*, 2006; 5: 578-88.
- Pollo C, Vingerhoets F, Pralong E, Ghika J, Maeder P, Meuli R, Thiran JP, Villemure JG. Localisation of electrodes in the subthalamic nucleus on magnetic resonance imaging. *J. Neurosurgery*, 2007; 106: 36-44.
- Psychological assessment resources. Computerized Wisconsin Card Sort Task Version 4 (WCST), 2003.
- Rodriguez-Oroz MC, Rodriguez M, Guridi J, Mewes K, Chockkman V, Vitek J, DeLong MR, Obeso JA. The
620 subthalamic nucleus in parkinson's disease: somatotopic organization and physiological. *Brain*, 2001; 124(9): 1777-90.
- Reitan RM. Validity of the Trail Making test as an indicator of organic brain damage. *Percept. Mot Skills*, 1958; 8: 271-6.
- Saint-Cyr JA, Trépanier LL, Kumar R, Lozano AM, Lang AE. Neuropsychological consequences of chronic
625 stimulation of the subthalamic nucleus in Parkinson's disease. *Brain*, 2000; 123: 2091-108.
- Saint-Cyr JA, Hoque T, Pereira LC, Dostrovsky JO, Hutchison WD, Mikulis DJ, Abosch A, Sime E, Lang AE, Lozano AM. Localization of clinically effective stimulating electrodes in the human subthalamic nucleus on magnetic resonance imaging. *J Neurosurgery*, 2002; 97(5): 1152-66.
- Schaltenbrand G, Wahren W. Atlas for Stereotaxy of the Human Brain. Thieme, Stuttgart, Germany, 1977.

- 630 Schwab RS, England AC. Projection techniques for evaluating surgery in Parkinson's Disease. Third Symp on Parkinson's disease, Edinburgh, Scotland, 1968; 152-7.
- Stancanello J, Muacevic A, Sebastiano F, Modugno N, Cerveri P, Ferrigno G, Uggeri F, Romanelli P. 3T MRI evaluation of the accuracy of atlas-based subthalamic nucleus identification. *Med Phys*, 2008; 35(7): 3069-77.
- Stroop JR. Studies of interference in serial verbal reactions. *Journal of Experimental Psychology*, 1935; 18: 643-62.
- 635 Talairach J, Tournoux P. *Co-Planar Stereotaxic Atlas of the Human Brain*. Thieme, Stuttgart, Germany, 1988.
- Temel Y, Kessels A, Tan S, Topdag A, Boon P, Visser-Vandewalle V. Behavioural changes after bilateral subthalamic stimulation in advanced Parkinson disease: a systematic review. *Parkinsonism Relat Disord*, 2006; 12: 265-72.
- Theodosopoulos PV, Marks WJ, Christine C, Starr PA. Locations of movement-related cells in the human subthalamic nucleus in Parkinson's disease. *Movement disorders*, 2003; 18(7): 791-8.
- 640 Troyer AK, Moscovitch M, Winocur G, Leach L, Freedman M. Clustering and switching on verbal fluency tests in Alzheimer's and Parkinson's disease. *J Int Neuropsychol Soc*, 1998; 4(2): 137-43.
- Volkman J, Albanese A, Kulisevsky J, Tornqvist AL, Houeto JL, Pidoux B, Bonnet AM, Mendes A, Benabid AL, Fraix V, Van Blercom N, Xie J, Obeso J, Rodriguez-Oroz MC, Guridi J, Schnitzler A, Timmermann L, Gironell AA, Molet J, Pascual-Sedano B, Rehncrona S, Moro E, Lang AC, Lozano AM, Bentivoglio AR, Scerrati M, Contarino MF, Romito L, Janssens M, Agid Y. Long-term effects of pallidal or subthalamic deep brain stimulation on quality of life in Parkinson's disease. *Mov Disord*, 2009; 24: 1154-61.
- 645 Witt K, Daniels C, Reiff J, Krack P, Volkman J, Pinsker MO, Krause M, Tronnier V, Kloss M, Schnitzler L, Wojtecki L, Bötzel K, Danek A, Hilker R, Sturm V, Kupsch A, Karner E, Deuschl G. Neuropsychological and psychiatric changes after deep brain stimulation for Parkinson's disease: a randomized, multicentre study. *Lancet Neurology*, 2008 ; 7(7) : 605-14.
- 650 Yelnik J, Bardinet E, Dormont D, Malandain G, Ourselin S, Tandé D, Karachi C, Ayache N, Cornu P, Agid Yves. A three-dimensional, histological and deformable atlas of the human basal ganglia. I. Atlas construction based on immunohistochemical and MRI data. *NeuroImage*, 2007; 37: 618-38.
- York MK, Wilde EA, Simpson R, Jankovic J. Relationship between neuropsychological outcome and DBS surgical trajectory and electrode location. *J Neurol Sci*, 2009; 287(1,2) : 159-71.
- 655 Zaidel A, Spivak A, Grieb B, Bergman H, Israel Z. Subthalamic span of beta oscillations predicts deep brain stimulation efficacy for patients with Parkinson's disease. *Brain: a journal of neurology*, 2010; 133: 2007-21.